Challenging Glass 6 - Conference on Architectural and Structural Applications of Glass
Louter, Bos, Belis, Veer, Nijsse (Eds.), Delft University of Technology, May 2018.
Copyright © with the authors. All rights reserved.
ISBN 978-94-6366-044-0, https://doi.org/10.7480/cgc.6.2149

Hybrid Steel-Glass Cell: Cold-twisting and Buckling Phenomena

Laura Galuppi [a], Pietro Di Biase [b], Benjamin Schaaf [b], Carl Richter [b], Benno Hoffmeister [b], Markus Feldmann [b], Gianni Royer Carfagni [a]

[a] *Department of Engineering and Architecture, University of Parma, Italy, e-mail laura.galuppi@unipr.it*
[b] *Institute for Steel Construction, RWTH Aachen University, Germany*

The European RFCS project "S+G" has developed innovative steel-glass composite systems for high-performance building skins, meeting requirements of structural and energetic efficiency, as well as aesthetical value and versatility of applications. The aim of the project has been the design, prototype and testing of unitized cells composed by a glass panel and a contouring metallic frame, twisted by cold bending into a hyperbolic paraboloid shape, to be used in free-form curved building façades. To achieve large curvatures while maintaining the stress under the limit strength, very thin glass needs to be used, with a consequent risk of loss of stability. Preliminary investigations have been conducted to evaluate the buckling load in the glass panel and the possible stiffening effect of the contouring metallic frame. Then, accurate FE analyses, accounting for geometric and material nonlinearities, have been used to optimize the design of the unitized cell. Finally, two-steps experimental tests have been performed on full-scale samples. First, the prototypes are cold-twisted, maintaining limited the displacement of the corners, so to avoid buckling. Secondly, out-of-plane loading is applied to simulate wind, snow or man load. Thanks to the curvature, the cells showed very high strength due to the synergetic coupling of steel and glass. Here, we present the experimental and numerical investigations and the main results from full-scale tests. These have been used to refine the FE model, in order to investigate the role of both the interlayer and of the steel-to-glass bonding, and to develop a simplified model for practical design applications.

Keywords: Steel-glass hybrid structure, cold bending, buckling, experimental tests, structural bonding, innovative joints.

1. Introduction

The most important technological achievements in modern architecture are attained by constructing smart building skins, usually by combining glass and metal to form the external envelope of a building, often called the "third skin". This delimits the indoor living space, controls the energy transfer between inside and outside by selective filtering of heat and light, and defines the aesthetic appeal of the building. As the demand for complex geometries and improved performance increases, innovative and non-uniform building envelope solutions have to be devised. Furthermore, the traditional curved glass obtained through hot-bending, a process in which heated glass rests on molds in a large kiln and takes its shape from them, is being replaced by cold-bent glass. *Cold bending* technique is increasingly developing because it does not need any negative template, leading to consistently lower costs with respect to hot bending since the degree of curvature can be easily modified through a slight variation of the constraining actions.

The aim of the European Research Fund for Coal and Steel (RFCS) project "Innovative Steel Glass composite structures for high-performance building skins" (Royer Carfagni *et al.*, 2016) has been the design, prototype and testing of innovative steel-glass composite cells, produced by cold bending, usable for free-form curved surfaces of building façades. The goal has been to achieve the synergetic composition of the two materials, using glass as a load-bearing material in association with steel. To this aim, glass and steel need to be structurally coupled with high-performance adhesives. With respect to classical cold-bending, where glass is inflexed and successively constrained to the frame, in this new concept-design the steel frame is connected to glass in the flat configuration and, afterwards, the whole cell is cold-bent. With this technique, smooth curved glazed surfaces can be obtained from the assembly of various cells with "large" production tolerances, since adjustments can be made directly *in situ*.

The hyperbolic paraboloid shape, a quadric surface shaped like a saddle (see Fig. 1), is of interest for this project because it can be simply obtained by *twisting*, i.e., through the action of four opposite concentrated forces at the plate corners, perpendicular to the plate itself. The advantage of this shape consists in the wide range of different surfaces that can be obtained through the repetition, with minor changes, of an elementary unit, as shown in Fig. 1, as well as to the ready applicability of the cold bending technique.

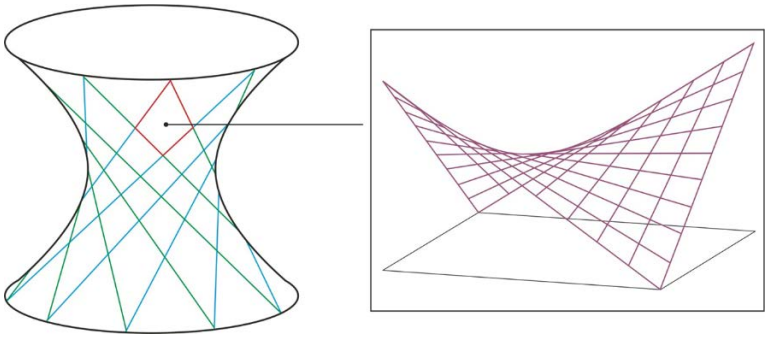

Fig. 1. A hyperbolic paraboloid shape.

Experimental tests and numerical simulations have provided evidence that, at a certain level of the applied actions at the corners, a little-known form of buckling occurs (see, among the other, the accurate and extensive experimental campaign recorded in (Datsiou, 2017)). For its description, an analytical non-linear model has been proposed to accurately estimate of the relationship between the applied forces and the displacements at the corners (Galuppi *et al.*, 2014). Numerical parametric analyses have allowed to calculate the buckling limit, over which instability arises, as a function of the glass thickness and of the aspect ratio of the panel. In a second phase, FEM analyses have been made on different solutions for the unitized steel-glass cell, presenting different degree of complexity (Royer Carfagni *et al.*, 2016). First, simulations were made to investigate the effect of cold-bending, accounting for the viscoelasticity of the interlayer and geometric non-linearity. Therefore, the response of unitized cells with the glass panel bonded to different-in-type metallic frames and with diverse structural adhesives, has been investigated. On the basis of these results, a simplified model has been developed for the engineering practice. Since a critical factor is the recognition of the precise stability limit of the unbuckled state, these results have been used to refine and optimize the cell geometry.

Finally, experimental tests have been performed on full-scale samples, by considering the different cell concepts, with three different structural adhesives. Each experiment includes two testing steps. First, the prototypes are cold-bent, with prescribed corners' displacement values, chosen to avoid instability phenomena in the glass plate and to obtain a hyperbolic paraboloid deformed shape after cold bending, also taking into account the beneficial stiffening effect of the metallic frame. Secondly, out-of-plane loading is applied to simulate wind, snow and man load.

2. Cold twisting and buckling

The Kirchhoff-Love theory of thin elastic plates predicts that the hyperbolic paraboloid shape, shown in Fig. 2a, can be obtained by applying four opposite concentrated out-of-plane loads at the plate corners. Sections of the deformed surface orthogonal to its reference middle plane and passing through the diagonals are two identical parabolas, with opposite concavities. Experimental results and numerical simulations by many authors (Beer 2013, Galuppi *et al.* 2014) have provided evidence that, at a certain level of the applied loads, a particular form of elastic instability occurs, where bending becomes predominant along one diagonal, rather than symmetric along the two diagonals (Fig. 2b).

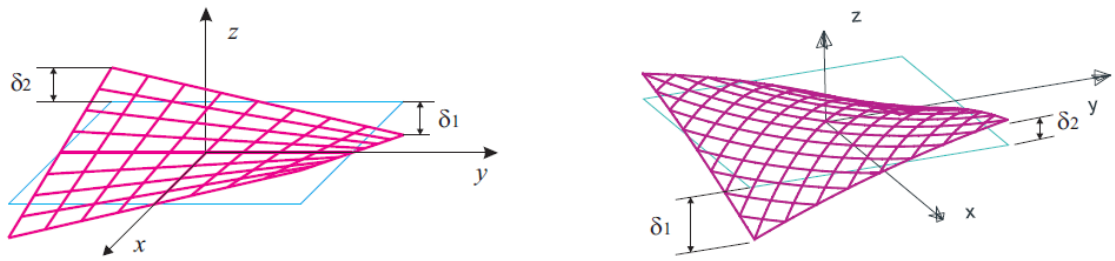

a) b)

Fig. 2 Cold-twisted square plate: a) hyperbolic paraboloid; b) asymmetric (buckled) configuration.

The buckling occurrence may be detected by measuring the relative displacements of the corners with respect to the center of the plate. With reference to Fig. 2, with respect to the undistorted (flat) reference configuration of the panel, let us denote with δ_1 the displacement of the points where the applied forces are directed downward, and by δ_2 the displacement (directed upwards) of the other corners. It is evident that, whenever the deformed shape is symmetric with respect to the diagonals, then $\delta_1 = \delta_2$; on the contrary, $\delta_1 \neq \delta_2$ characterizes the onset of asymmetrical configurations associated with almost-unidirectional bending. Another equivalent way to detect the onset of instability is to measure the out-of-plane displacement of the plate center with respect to its position in the reference configuration.

The *buckling limit* may be conventionally defined as the maximum displacement of the corners that can be assigned to obtain an out-of-plane displacement of the plate center of less than 1 mm.

2.1. Analytical modelling

In (Galuppi *et al.*, 2014), a simple analytical nonlinear model has been presented, based on inextensional theory for thin flat plates. It allows to describe, albeit qualitatively, the response of plates under twisting, accounting for geometric non-linearities that come into play when the prescribed corner's displacement cannot be considered "small" with respect to the plate size. This approach gives an estimation of the corners' constraint reactions as a function of the prescribed displacements that is in good agreement with the numerical results, as shown by Fig. 3a, where we compare the results, in terms of load-displacement response, obtained through the proposed model, either non-linear or linear (Kirchhoff-Love theory for plates). The considered paradigmatic case is a square monolithic glass plate with thickness 10 mm and edge length of 2 m; Young's modulus and Poisson's ratio are 70 GPa and 0.22, respectively. The numerical analyses, accounting for geometrical non-linearities, have been performed in Abaqus, by using a 3-D mesh with solid 20-node quadratic bricks with reduced integration, referred to as C3D20R in the Abaqus library. The structured mesh has been created by dividing the length of each plate edge in 50 elements and its thickness in 3 elements.

To enhance the rate of convergence of the numerical computations, the asymmetric configuration has been "promoted" by slightly "pushing" the plate in the out-of-plane direction. The FE analyses have been performed in three steps: first, a uniformly distributed pressure p=10-3 MPa has been applied; afterwards the plate corners have been displaced up to the target value; finally, the load *p* has been removed. In the practical case of a real building glazing, the effect of *p* could be associated with the self-weight (for horizontal panels) or to action of wind or snow (for vertical panels).

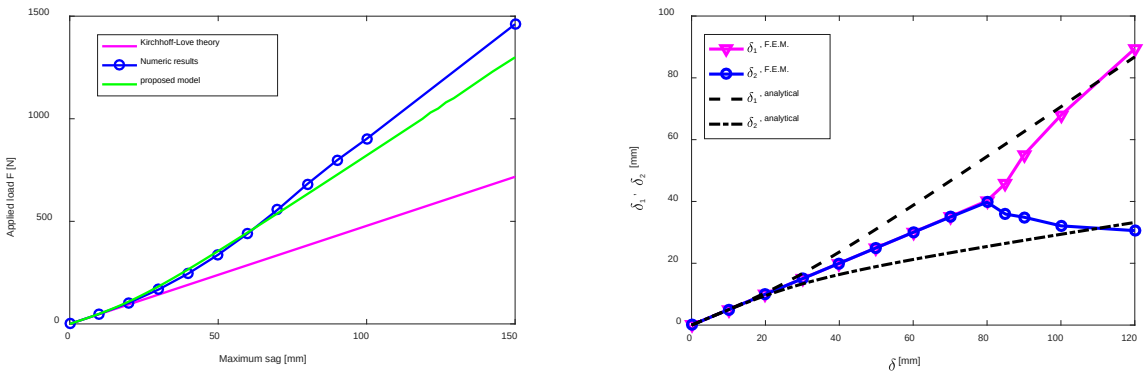

a) b)

Fig. 3 a) Comparison of the force vs. displacement graphs obtained through the linear analysis (Kirchhoff-Love), the model proposed in (Galuppi *et al.*, 2014) and the FEM simulations; b) Displacements δ1 and δ2 as functions of δ. Analytical and FEM results

The proposed model, despite its simplicity, allows to evaluate the displacements δ_1 and δ_2 at the corners and, consequently, to measure of the "asymmetry" of the deformation. It is evident from Fig. 3b that, even if the analytical model cannot predict the onset of the instability, it gives results that are in good qualitative agreement with the numerical ones. For large displacement, the numerical and analytical values tend to coincide.

2.2. Influence of geometric parameters on buckling

The onset of buckling is strongly influenced by the plate geometry (edge lengths and glass thickness), as well as by the laminated package composition in the case of laminated glass. Remarkably, depending on the plate thickness, size and aspect ratio, instability may occur before or after that the glass reaches its limit strength. To illustrate, consider a square 2 m x 2 m glass plate and a 1 m x 2 m rectangular plate, both four-point supported and with thickness 10 mm. Fig. 4a and Fig. 4b show the displacement δ_1 and δ_2 for these two cases, respectively, as functions of the prescribed corners' displacement δ, evaluated through numerical analyses performed in Abaqus, as described in the previous section. Furthermore, in the same graphs the value of δ for which the maximum stress in the glass ply is of the order of 50 MPa is marked with a dashed line.

By comparing Fig. 4a and Fig. 4b, it is evident that a different-in-type behavior may be recognized in the two cases: for the square (2 m × 2 m) plate, instability occurs before that the glass reaches its limit strength, whereas for the 1 m × 2 m plate, the limit strength of the material is reached before the buckling limit.

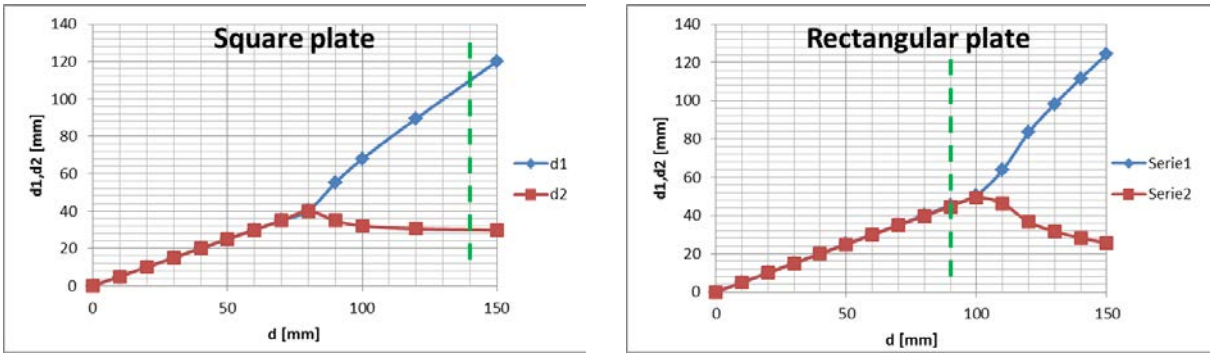

a) b)

Fig. 4 Four-point supported glass plate. Displacements δ_1 and δ_2 as functions of the prescribed total displacement δ. a) 2 m × 2 m and b) 2 m × 1 m glass plate, 10 mm thick.

To investigate the influence of geometric parameters on the arising of the instability, the case of four-point supported rectangular plates of size $a \times b$, made of monolithic glass of thickness h, is here considered here. Fig. 5a and Fig. 5b shows the buckling limit for a monolithic glass plate, 8 mm and 12 mm thick, respectively, as a function of the plate edge lengths a, b=1 ÷3 m. Graphs have been obtained by means of a numerical parametric analysis performed with Abaqus, accounting for geometric nonlinearities. Again, the numerical analyses have been performed using a 3-D structured mesh with C3D20R elements.

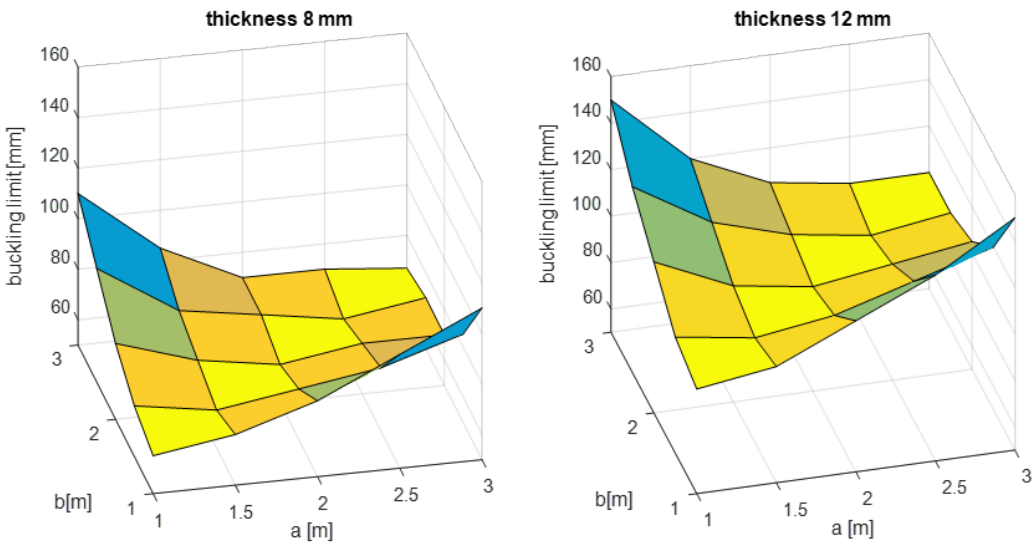

a) b)

Fig. 5 Four-point supported glass plate. Buckling limit as a function of the plate edge length, for different plate thickness.

It is evident that the buckling limit is higher for high values of aspect ratio $\lambda = a/b$ (i.e., for rectangular plates) and, as expected, for high values of the plate thickness. Fig. 6 shows the buckling limit, plotted as a function of the glass thickness and of the aspect ratio $\lambda = a/b$, for different plate length a. These charts may be used as a practical tool for preliminary design of glass panels cold-bent into a hyperbolic paraboloidal shape.

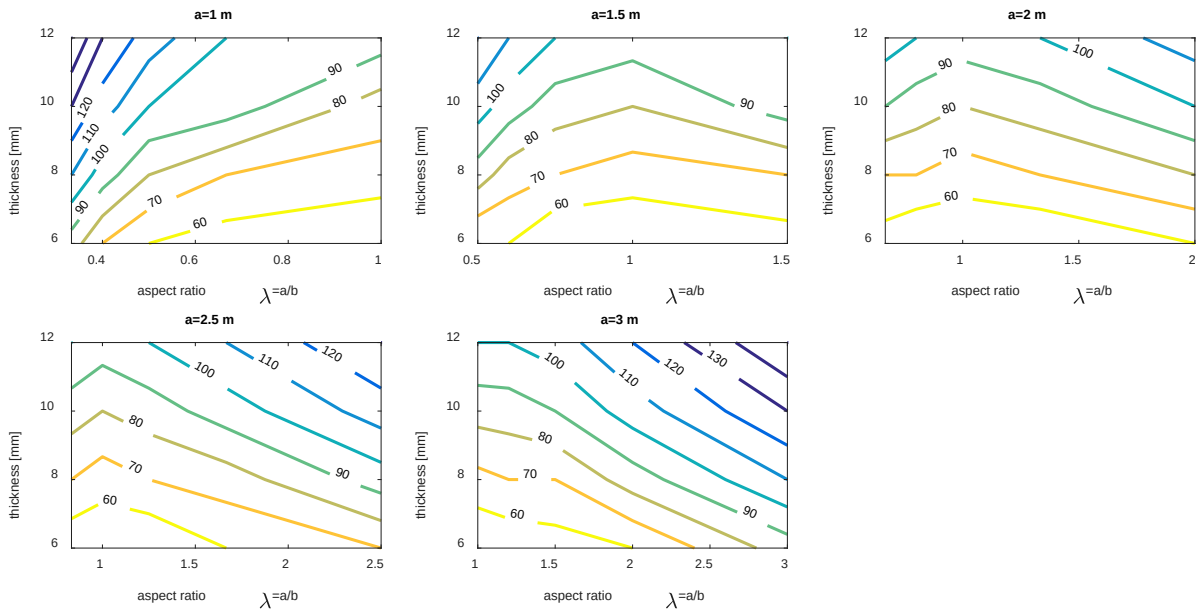

Fig. 6 Four-point supported glass plate. Buckling limits for different plate size, aspect ratio and thickness.

The response to bending of laminated glass is strongly affected by the presence of the polymeric interlayer that partially constrains the relative sliding of the constituent glass plies. As a first approximation, the Enhanced Effective Thickness (EET) method for plates (Galuppi *et al.*, 2013), allowing to evaluate the thickness of a monolithic glass with equivalent bending properties, may be used to study the stability of cold-bent laminated glass. However, since the EET method is calibrated for the case of small displacements and linear behavior, it is strongly recommended to evaluate the buckling response by performing numerical analyses on the laminated glass geometry.

2.3. Stiffening effect of the metallic frame

Notice that the buckled configuration of the plate is characterized by the curvature of the borders, whereas they remain straight when the deformation is small (Fig. 2a). Hence, a practical solution to increase the stability range and delay the buckling phenomenon is to stiffen the plate edges with a metallic frame (Royer Carfagni *et al.*, 2016). This allows to increase the amount of deformation of the cell and, thus, to obtain surfaces with higher curvatures.

An extensive campaign of numerical experiment has been performed to determine the stability limit of the glass plate with rigid edges, supposing that the action of the frame is equivalent to a perfect constraint, compelling the glass borders to remain perfectly straight while the whole cell is twisted. The geometry and mesh considered in the FEM analyses is the same described in the previous sections. The presence of the rigid frame has been simulated by prescribing, at the points belonging on the plate edges, displacement linearly varying along the edge itself.

Graphs in Fig. 7 show the buckling limit as a function of the glass thickness and of the plate aspect ratio, for different plate size. By comparing Fig. 7 with Fig. 6, it is possible to verify that the stiffening effect of the metallic frame increases the buckling limit of the plate. For example, by stiffening the edges of a 1.5 m × 3 m plate, 8 mm thick, the buckling limit can be increased from 85 mm to 130 mm.

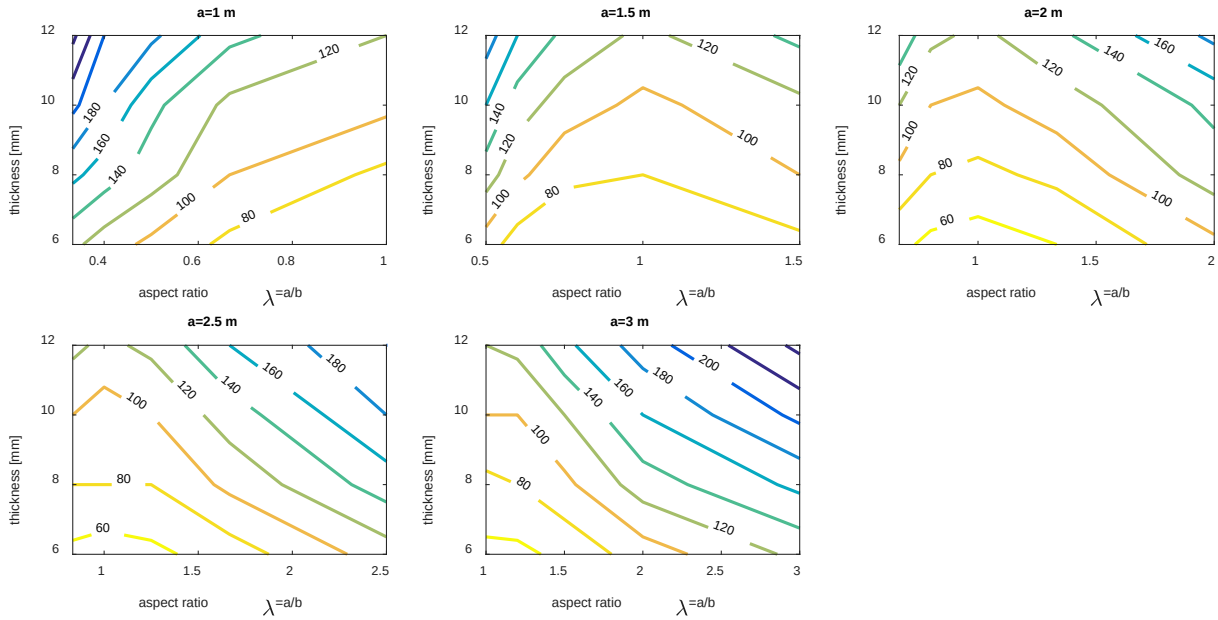

Fig. 7. Plate with rigid edges. Buckling limits for different plate size, aspect ratio and thickness.

3. Numerical and experimental analysis of cold-twisted hybrid cells

3.1. Validation of FE models based on experimental investigations

The following Section presents the most important results of the accompanying FE calculations. Based on the experimental data, numerical models are created with ANSYS 18.1 Classic. The specimens were modelled with three-dimensional continuum elements, which are stored in the element library. In the APDL (Ansys Parametric Design Language) each of them is determined with a unique item number, like 185 for Solid185 (8-node hexaedral-element) or 186 for Solid186 (20-node hexaedral-element). The element types differ mainly in their shape and in their functions. Due to the fact that the adhesive has the function of the bond between the steel frame and the glass panel, the discretization was made with the structural elements Solid186. Although the choice of Solid186 elements causes a higher computational effort, there is the advantage of getting a better quality of the computational results. The steel frame and the glass panel were discretized by Solid185 elements. The merging between the adhesive and steel frame and between the adhesive and the glass panel was defined by a contact definition with Target170- and Conta173-elements. For the adhesive, the hyperelastic Mooney-Rivlin model was used. For the other components linear elastic material behaviour was assumed. The system was loaded with self-weight, the twisting and the external loading (pressure or suction). Using appropriate contact definitions as well as corresponding material and geometric parameters, the hybrid cell is completely modelled. Subsequently, convergence studies are carried out. Linear material models are used for the materials (steel, PVB and glass), whereas for the adhesive we use a hyperelastic two-parameter Mooney-Rivlin model (Rivlin 1948). Geometric non-linear effects are taken into account, since it cannot be ruled out that they may have an unfavourable influence on the design of glass due to cold bending (DIN 18008: 2010).

The numerical simulation is divided into two load steps, analogous to experimental tests (Hoffmeister *et al*. 2016). First, the desired shape is reached by cold bending; then the actual load (pressure/suction) is applied to the glass pane. The deformed shapes correspondent to each load step are shown in Fig. 8.

Fig. 8 Load step I: cold bending (left), load step II: cold-bent model under pressure load (right).

Fig. 9 exemplarily compares the load-displacement curve of the FE calculations with experimental data of a line supported (this configuration rules our instabilities) hybrid cell (Hoffmeister *et al*. 2016, Royer-Carfagni *et al*. 2016, Caprili *et al*. 2017), bonded with DC993 adhesive, under pressure load. There is a very good agreement between

simulations and tests. With the help of the FE model, calibrated to match the test data, further investigations are carried out.

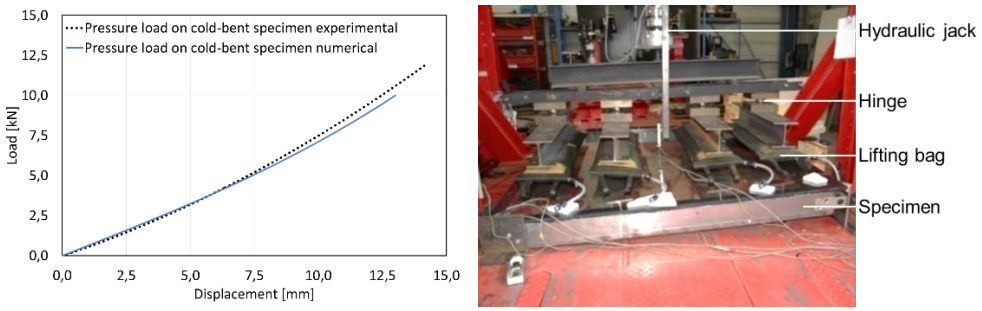

Fig. 9 Comparison experimental data and simulation for a cold-bent hybrid cell under pressure load (left), test setup (right).

3.2. Analysis of cold bending

With the calibrated FE models, further investigations on the influence of cold bending and shear bond on glass and adhesive can be performed. Fig. 10 shows the resulting symmetrical distribution of the first principal stress in the glass, as well as the von Mises strain in the adhesive: this refers to the unloaded state after cold bending for a full shear bond of the laminated glass, a condition that has to be considered according to (DIN 18008 2010). The maximum stress (approximatively 30.8 MPa) in glass occurs in the middle of the edge (this is approximatively 40% of the design strength of safety glass). The maximum strain resulting from the restoring forces in the adhesive (approximatively 0.12) are located in the corner area and lead to stresses which are above the design value according to (ETA 2012).

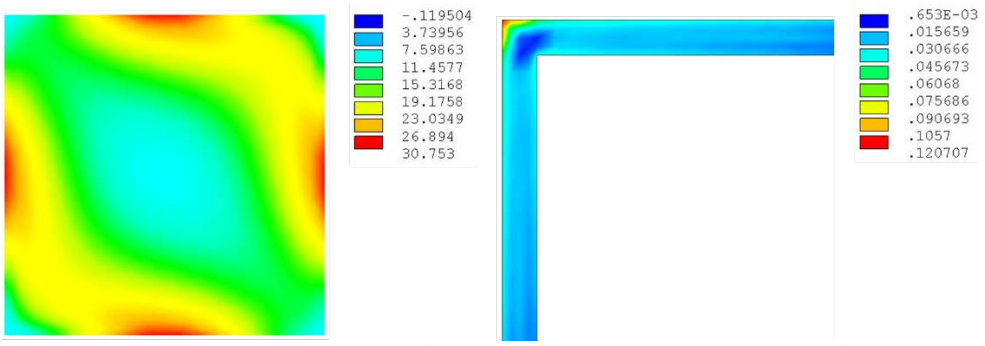

Fig. 10 First principal stress distribution in the glass (left) and von Mises strain in the adhesive (right) after cold bending

In order to examine a practical case, typical design actions for wind suction according to (Kasper *et al.* 2016) are applied for the ultimate limit state of load capacity (ULS) or serviceability limit state (SLS). The influence of cold bending on the load-induced stresses in the glass can be determined. Fig. 11shows the state of stress in glass for a flat (left) and a cold-bent panel (right), without taking into account the additional stresses resulting from cold bending. These are expected to be maximum for both cases in the middle of the plate. For flat glass, the load-induced stresses of 11.8 MPa are significantly higher than for the cold-bent glass (3.3 MPa).

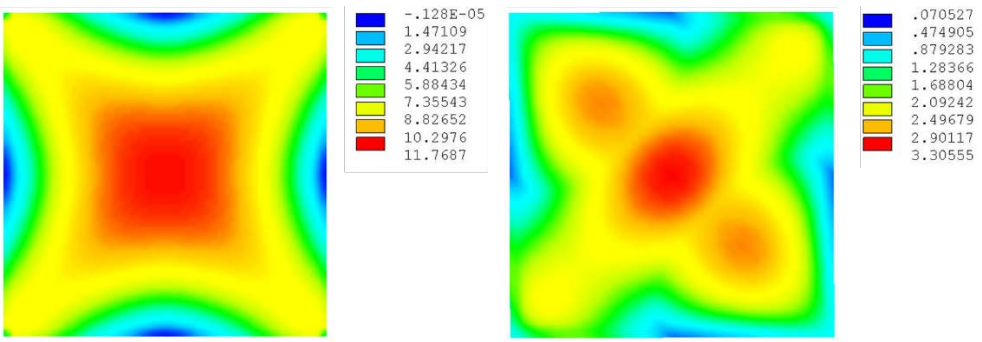

Fig. 11 Comparison of the principal tensile stress of a flat (left) and cold-bent (right) glass panel, for the ultimate limit state of the load-bearing capacity

In superposition with the stresses from cold bending, the stresses in the middle remain at the same low level compared to the flat glass since here the effect of cold bending is null. However, the most critical state of stress is found in the middle of the edge (32.6 MPa). This is about 2.5 times higher than for the case of flat glass.

3.3. Analysis of the shear bond of the laminated glass

The influence of viscoelastic effects is now considered. In addition to the viscoelastic behavior of the adhesive, which absorbs the restoring forces of the cold bending process and is thus exposed to relaxation, also the PVB interlayer of the laminated safety glass is also stressed and relaxed by the cold bending process. The mathematical description of the viscoelastic material behavior of adhesives is a subject of current research. The time- and temperature-dependent response of the PVB interlayer is already much more investigated (Langosch *et al*. 2013). The time-dependent parameter of importance is the shear modulus G of the interlayer. This is set to be G_0= 0.4 MPa for time t = 0 and G_∞ = 0.052 MPa for $t = \infty$ to (Wellershof *et al.* 2007). To illustrate the influence of the viscoelasticity of the PVB interlayer, in Table 1 we record for various values of G the deflection $w_{d,max}$, the stress acting in the middle of the glass plate $\sigma_{d,Mid}$ and the maximum stress $\sigma_{d,max}$. In addition, the maximum design loads $F_{d,max}$ (lifting forces at the corners) to be applied by the substructure are given. From values in Table 1, it becomes clear that for cold-bent glass, a design based on the assumption that there is no shear bond is unsafe. Therefore, as also stated by (DIN 18008:2010), an additional limit value analysis with full composite (monolithic) response shall be carried out for the design, on the safe side. If the partial bond is used, as described in (Langosch *et al*. 2013), the design values are reduced again. The thickness of the shear bond has a minor effect on the maximum stress occurring in the glass due to the cold bending. However, the influence on the stress in the middle of the glass plate is considerably higher. The influence of the relaxation of the interlayer on the load-bearing capacity at the ULS can also be assessed positively, as the stresses are reduced. In return, however, this influence has a negative effect on the serviceability limit state as the deformations increase.

Table 1 Stresses, deformations and loads calculated with FEM for ultimate limit state

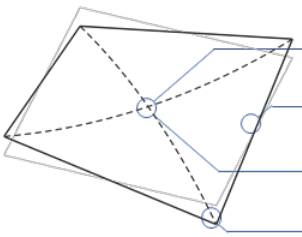

VSG 66.4	No shear bond G=0 MPa[1]	Partial shear bond G=0,052 MPa	Partial shear bond G=0,4 MPa	Quasi full shear bond G=50 MPa
$\sigma_{d,Mid}$[2] [MPa]	1,8	2,2	7,2	11,9
$\sigma_{d,max}$[2] [MPa]	31,0	31,4	31,7	32,6
$w_{d,max}$ [mm]	3,7	3,0	2,8	2,0
$F_{d,max}$ [kN]	2,0	3,4	3,7	5,3

[1] Design with no shear bond based on (DIN 18008 2010) with equivalent thickness
[2] Stresses on the loaded side of the laminated safety glass

4. Numerical model for practical applications

Relying upon the experimental data, numerical models were created with ANSYS 18.1 Classic. These models are characterised by a realistic description of the testing conditions, which include the simulation of all materials (glass, PVB, adhesive, steel) and the consequential arising issues. The fundamental idea of this Section is the reduction of the computational effort while maintaining the accuracy of the previously created models. In this way, it is possible to create a practical tool, which enables a cost-effective solution through a much lower calculation duration.

For the purpose of validation, in a first step the numerical results are compared with the experimental data (see Sect. 3). The comparison confirms that these complex numerical models are able to simulate the experimental tests with a very adequate consistency. In order to reduce the computational time, these complex models are simplified by considering the cold bending process as an *increased overall glass stiffness*. Additionally, the adhesive is substituted by equivalent spring elements. It is necessary to ensure that the numerical results are not deteriorated within the process of simplification. Therefore, the outcome of the newly developed models are compared with the results of the complex models. If the quality of results of the simplified models is ensured to be as accurate as the complex models, they can be used for further investigations. In the following, the used element technologies, finite elements structure and experimental as well as numerical results are illustrated (see Fig. 12).

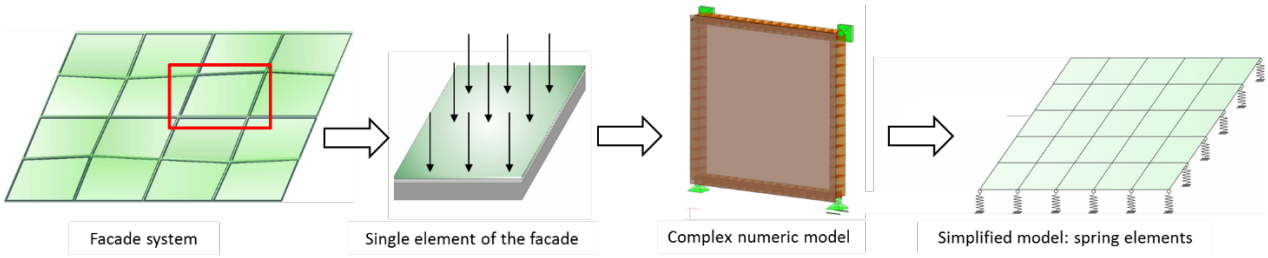

Fig. 12 Numerical evaluation scheme.

Due to the simplifications, slight deviations have to be accepted. There are various options to reduce complexity of numerical models as, for instance, coarsening meshes, using low-order elements or neglecting geometric non-linearities. These simplifications do reduce the computational effort but, adversely, affect the quality of the numerical simulations, which ultimately lead to incorrect results. Therefore, a more efficient way of reducing the complex models has to be found.

The current calculation routine of the numerical models is divided into two separate processes. First, the flat glass panel is cold-bent and the resulting deformations are calculated. In a second load step the geometry of the model is updated to the previously calculated cold-bent state and the load (pressure or suction) is applied followed by a second solution process. The cold bending of the glass panel has a positive effect on the stiffness of the panel regarding the out-of-plane loads (pressure or suction), that can also be observed through the numerical simulations. The first step of simplifying the numerical model is to renounce the cold bending process by an equivalent glass stiffness resulting from the actual cold bending, which is done by modifying the modulus of elasticity with an equivalent stiffness factor. This is determined as the ratio between the initial stiffness of a flat glass panel and that of the cold-bent panel, under experimental load. Instead of simulating the cold bending process, the Young's modulus of the flat glass is multiplied by this factor, to account for the increasing stiffness resulting from the cold bending. Fig. 13 shows that these simplifications provides results very similar to those obtainable with the original complex model (red curve). In this way, the simulation of the cold bending can be neglected, which saves about 50% of the calculation time.

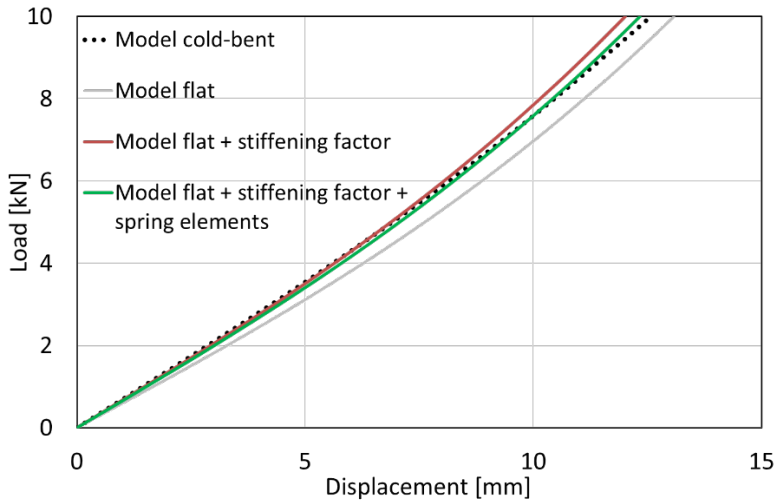

Fig. 13 Comparison of different numerical models under pressure: global response.

Furthermore, the frame and the adhesive, as well as the associated complex contact elements, are simplified in a second step. Only the glass panel is modelled by high-order shell elements, while the adhesive is substituted by spring elements, located at the outer edge of the panel. The corresponding equivalent spring stiffness is determined by

$$c_{adh} = \frac{EA}{d} \tag{4.1}$$

where E is the Young's modulus, A the cross section and d the thickness of the adhesive. To simulate the adhesive layer, several spring elements have to be used. Due to the geometric boundary and loading conditions, the spring elements are connected in parallel. This implies that the spring stiffness of each spring element is equal to the total spring stiffness divided by the actual number of used spring elements, which depends upon the chosen mesh. The frame is considered by trying to impose equivalent boundary conditions. Fig. 14 gives an overview of the simplified numerical model.

Structural element	Element technology
Glass panel	SHELL181
Adhesive	COMBIN14

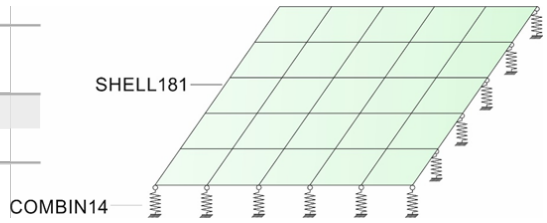

Fig. 14 Simplified numerical model using spring elements.

Fig. 13 also illustrates the results of this second simplification. The dotted black curve represents the load-displacement response of the complex numerical model, which is validated by the experimental data, and is used as the basis for investigations of the simplified models. The numerical results obtained by considering the planar glass panel (without the stiffness increase due to cold-bending) is shown by the grey curve. By multiplying the glass stiffness by the effective stiffness factor – as outlined before – the red curve is obtained. This numerical model somewhat overestimates the basic model for high values of displacement. As a last step, the spring elements are applied as shown in Fig. 14 and the correspondent result is plotted in the graph with the green curve. The global behavior of this model shows the least differences in comparison with the base model.

The substitutions from a complex model to a simplified model yield to nearly the same results. A major advantage of the simplified model is an improved handling and an enhanced calculation time. The same simplification is also performed for the suction load case, and leads to very similar results.

5. Conclusions

Hyperbolic paraboloid glazing for free-form building facades may be obtained through cold-bending of planar rectangular units, by forcing their corners in out-of-plane direction. Increasing the distortion, an instability phenomenon may be recognized: the plate achieves an asymmetric configuration, in which the bending occurs mainly about one of the two diagonal lines. Since the post-critical buckled configuration of the plate is characterized by the curvature of the borders, bonding the glass panels to a stiff contouring metallic frame may be regarded as a practical solution to increase the stability range and delay the buckling phenomenon. An extensive campaign of numerical experiment has been performed to determine the improvement of buckling limit obtained in this way.

This analysis has been the basis for the evaluation of the response of steel-glass hybrid cells, where the synergic action of the two materials is achieved through a structural bonding. Refined numerical investigations, accounting for material and geometric non linearities, show that the global response of a line-supported cold-bent element can be calculated very accurately, achieving very good agreement with experimental results. Numerical and experimental tests have demonstrated that the synergetic combination of the two materials outperforms more traditional glazing solutions, because glass is not just an infill panel, but it collaborates with the contouring steel frame to increase the load bearing capacity. Furthermore, thanks to the curvature, the panel can outstand out-of-plane loads better than a planar element. This proves the decisive influence of the cold bending on the cell response.

With the models calibrated from experiments, further investigations of the influence of cold bending and shear bond on glass and adhesive are carried out. The maximum stress in glass can be found in the middle of the edges also under the design actions, being more than twice as high as in the middle of the glass. For what concerns the adhesive, the highest strains result after cold bending. Relaxation of the laminated glass interlayer (PVB) plays a noteworthy role. Following the recommendation by (DIN 18800:2010), both the cases of full shear bond (monolithic limit) and no shear bond (layered limit) must be taken into account. The stresses are highest for the full shear bond, but the deformations are maximum in case of no shear bond.

Finally, a method for practical design is outlined by simplifying complex and time-consuming FE models. The investigation shows that this is possible by replacing the cold-bent panel by an equivalent flat glass panel with increased stiffness, and replacing the adhesive layer with spring elements. In this way, the calculation time can be drastically reduced, while maintaining a sufficient accuracy.

References

Beer, B., 2013. Complex geometry façades – Introducing a new concept design for cold-bent glass. In: Proceedings of Glass Performance Days, Tampere (Finland).

Caprili, S., Mussini, N., Salvatore, W. An innovative solution for hybrid steel-glass self-bearing modular systems. J Constr Steel Res 130,159-176 (2017).

Datsiou, K. Design and Performance of Cold Bent Glass. PhD Thesis, University of Cambridge (2017).

DIN 18008-1: Glas im Bauwesen – Bemessungs- und Konstruktionsregeln – Teil I und Teil II. Dezember 2010

ETA-01/0005, Sealant used in structural sealant glazing systems to bond glass onto metal, DC993 and DC895, 2012

EOTA: ETAG 002 - Guideline For European Technical Approval For Structural Sealant Glazing Kits (SSGK), 1040 Brussels, Belgium, June 1998

Langosch, K., Feldmann, M., Hoffmeister, B.: Wandartige Monoglasstützen unter axialen Drucklasten und Biegung, Stahlbau 82, 143-155 (2013).

Galuppi, L., Manara, G., Royer-Carfagni, G.: Practical expressions for the design of laminated glass. Comp. Part B – Eng. 45, 1677–1688 (2013).

Galuppi L., Massimiani, S., Royer-Carfagni G.: Buckling phenomena in double curved cold-bent glass, International Journal of Non-Linear Mechanics 64, 70–84 (2014).

Hoffmeister, B., Di Biase, P., Richter, C., Feldmann, M.: Innovative steel-glass components for high-performance building skins: testing of full-scale prototypes. Glass Struct Eng (2017) 2: 57. DOI 10.1007/s40940-016-0034-1

Kasper, R., Pieplow, K., Feldmann, M.: Beispiele zur Bemessung von Glasbauteilen nach DIN 18008, Verlag Ernst & Sohn, Berlin, 2016

Rivlin, R. S.: Large elastic deformations of isotropic materials. IV. Further developments of the general theory. Philosophical Transactions of the Royal Society of London Series A. Mathematical and Physical Sciences 241(835), 379–397 (1948).

Royer-Carfagni, G. *et al*., 2016. Innovative Steel Glass composite structures for high-performance building skins (S+G), Research for Coal and Steel (RFCS), Project RFSR-CT-2012-00026. Final Report.

Wellershoff, F.: Bemessungsschubmodulwerte für Verbundglasscheiben, Stahlbau 76, 177-188 (2007).